ADVANCED MATERIALS TECHNOLOGIES

Supporting Information

for *Adv. Mater. Technol.*, DOI: 10.1002/admt.201900563

Developable Rotationally Symmetric Kirigami-Based Structures as Sensor Platforms

*Erin E. Evke, Dilara Meli, and Max Shtein**

Developable Rotationally Symmetric Kirigami-Based Structures as Sensor Platforms

*Erin E. Evke[1], Dilara Meli[1], Max Shtein[1]**

[1] Department of Materials Science and Engineering.
* Corresponding author. Email: mshtein@umich.edu

Supplementary Materials

Supplementary Text

To further illustrate the deformation behavior of RSK spring, a ring model is created (**Figure S8**). The RSK spring is modeled as rings in series defined by its outer and inner radius (R_o and R_i) where the difference is the radial spacing. The applied concentrated force and pinned boundary conditions correspond to the uncut arc length designated by the cut pattern. The outer edges of the uncut regions of each ring are bounded by the previous ring, while the inner edges experience the load. Concentrated point loads are applied at the ends of each of the cuts, so for the baseline pattern that has two cuts along the circumference there are a total of four concentrated load points, assuming the forces are distributed equally. Therefore, the total force the ring experiences is the summation of the concentrated point loads where the force versus displacement plot represents the concentrated force at one of the cuts. Assuming each ring experiences the same applied load, the total displacement of the RSK spring is a sum of the individual displacements of each ring.

Analytical model

Cantilever beam theory can be used to describe the elastic behavior of the RSK springs, in which the global structure can be discretized as a series of rings. For a cut pattern having two cuts along the perimeter, the saddle-shaped rings can further be partitioned into eight beams based on the curvature of the ring, see **Figure S6**a. In other words, one cut segment can be decomposed to four beams where the force applied to one beam is one eighth the total force. The variables used for the derivation are the following:

δ: Deflection (mm)

F: Force (N)

R: Outer Radius (mm)

N_{pc}: Number of cuts along the perimeter

φ: Angular spacing (^{o})

S: Arc length (mm)

E: Young's modulus (N/mm^2)

w: Radial spacing (mm)

t: Thickness (mm)

E: Young's modulus (N/mm^2)

I: Area moment of inertia (mm^4)

N_{rings}: Number of active rings

x: Hinge length (mm)

Displacement of beam in bending fixed to one end:

$$\delta = \frac{FL^3}{3EI}$$

Where the area moment of inertia (I):

$$I = \frac{wt^3}{3}$$

The length of the beam corresponds to the arc length of the cut. The arc length based on the angular spacing:

$$S = 2\pi R\left(\frac{\theta}{360}\right)$$

$$\theta = \frac{360}{N_{pc}} - \varphi$$

$$L \equiv S = \pi R\left(\frac{2}{N_{pc}} - \frac{\varphi}{180}\right)$$

Therefore, the displacement of one beam:

$$\delta_{beam} = \frac{\left(\frac{F}{8}\right)\left(\frac{S}{4}\right)^3}{Ewt^3}$$

$$\delta_{total(i)} = 2\delta_{beam}$$

$$\delta_i = \frac{FS^3}{256Ewt^3}$$

The total displacement is the summation of each individual ring's displacement:

$$\delta_{total} = \sum_{i}^{N_{rings}} \delta_i$$

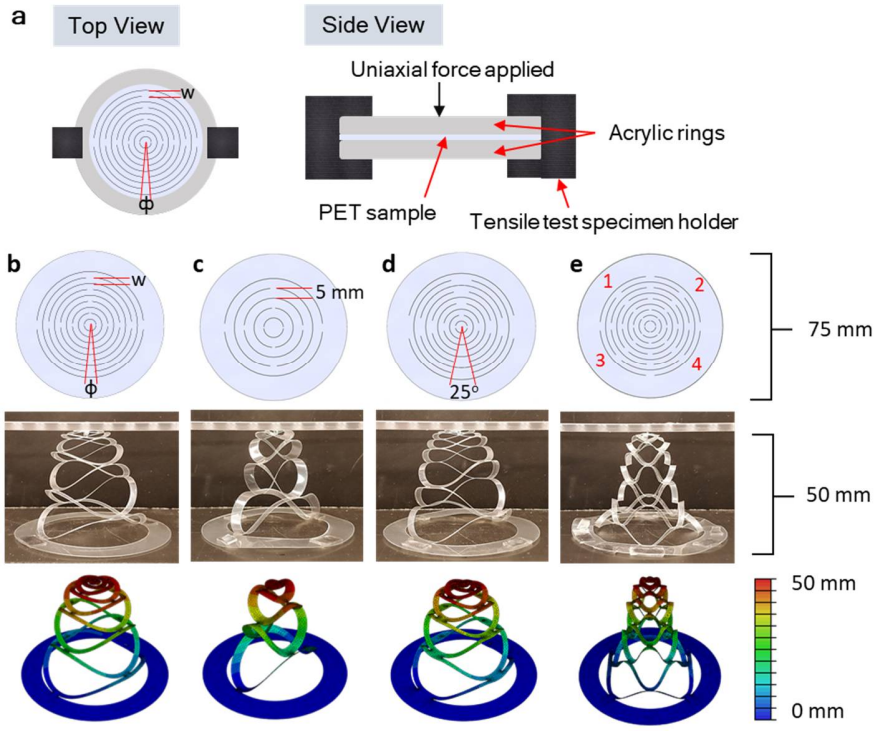

Figure S1. Experimental setup and comparison of experimental and FEA models displaced 50 mm. Each section is broken up into three rows where the top is a schematic illustration of the cut pattern used to fabricate RSK springs, the middle is the side view of the experimental springs, and the bottom is the FEA result. a) is the baseline pattern and (c)-(e) vary in the radial spacing (w), angular spacing (ϕ), and number of cuts along the perimeter (N_{pc}).

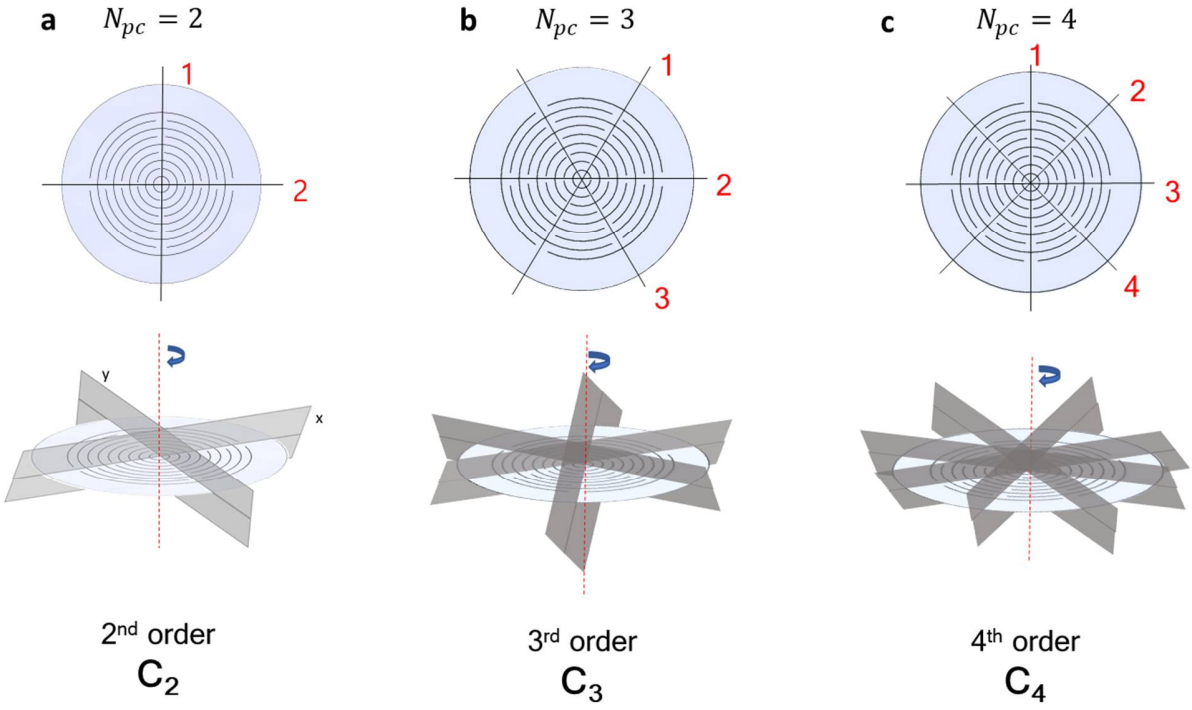

Figure S2. Order of rotational symmetry defined by the number of cuts along the perimeter. a) Second order, b) third order, and c), fourth order rotational symmetry.

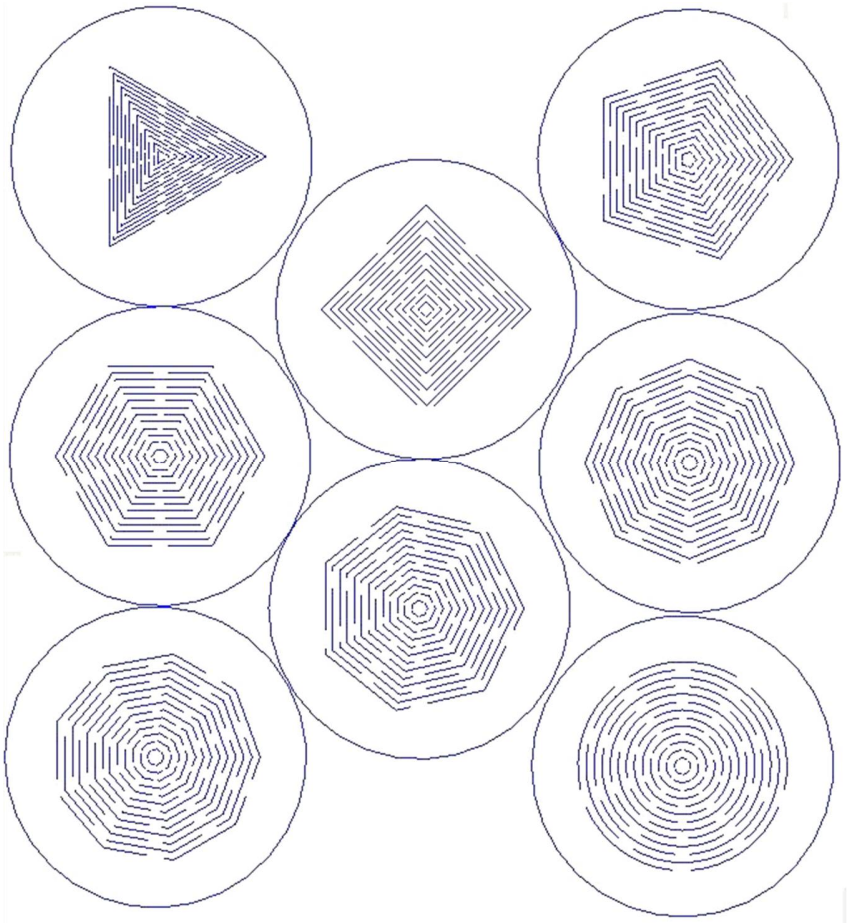

Figure S3. Examples of various shaped cut patterns having rotational symmetry.

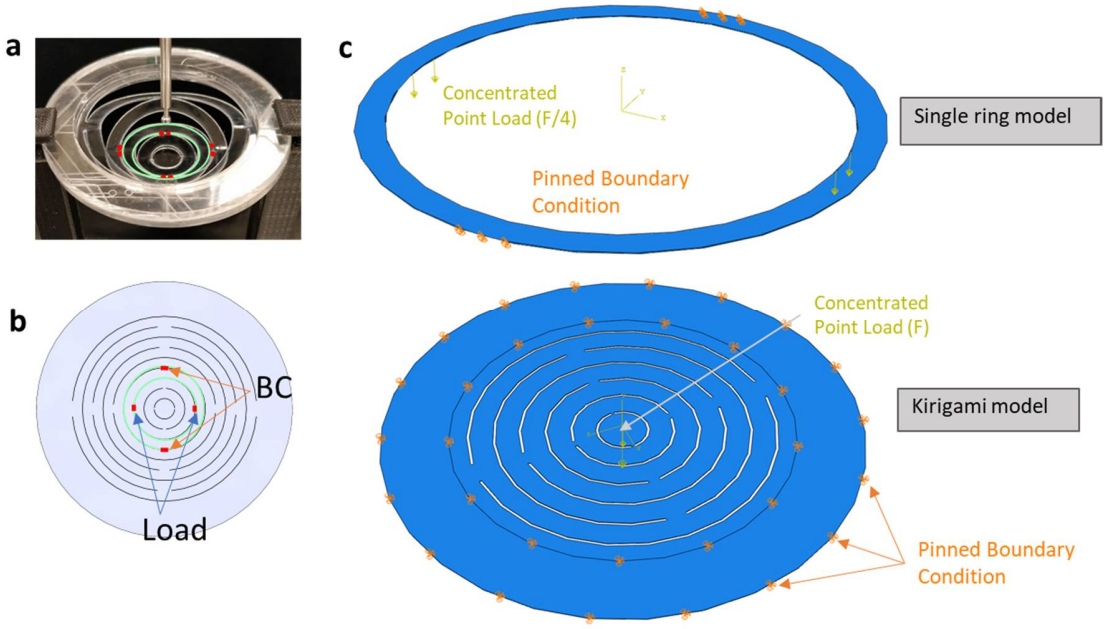

Figure S4. Setup of FEA simulations. a) An example of a sub-unit ring as the structure is deformed and (b) the respective highlighted ring depicting the inner ring experiencing the load and the other ring is bound. c) FEA load and boundary conditions setup with single ring model on top and the kirigami model below. Concentrated point loads are applied at the start of the cut at the inner part of the ring and the region between the cuts on the outer ring have a pinned boundary condition. The load for the kirigami model is applied at the center and a pinned boundary condition is applied on the outer ring.

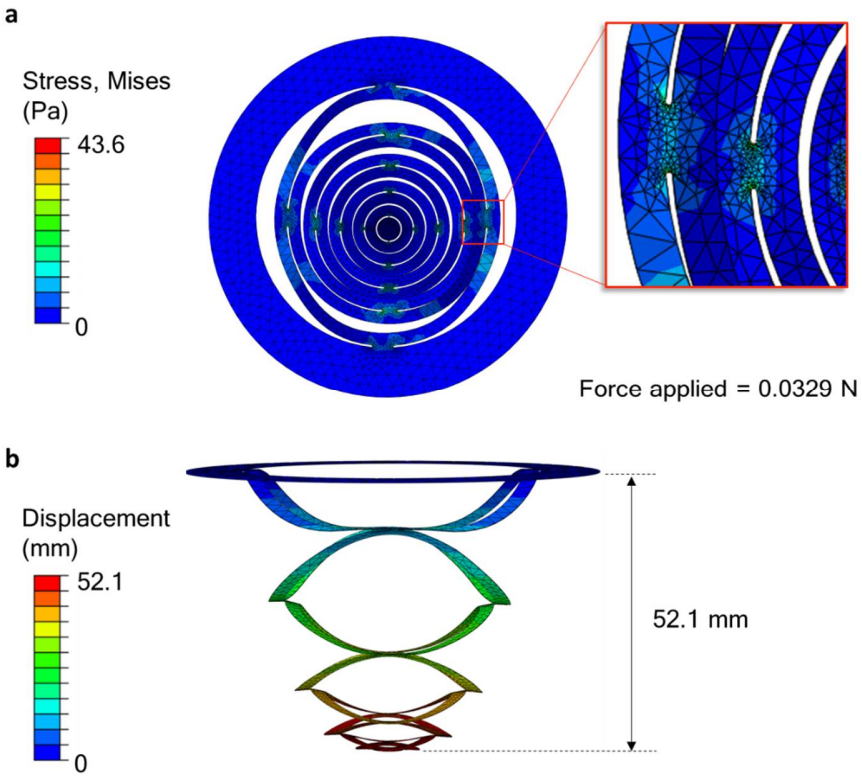

Figure S5. Stress and displacement of FEA simulations. a) Top view of deformed spring depicting the distribution of stress across the spring, based on Von Mises Criterion, where the scale bar is in Pa. The close-up is of the concentration of stress at the cut ends. b) Side view of deformed spring, where the color bar indicates displacement in mm.

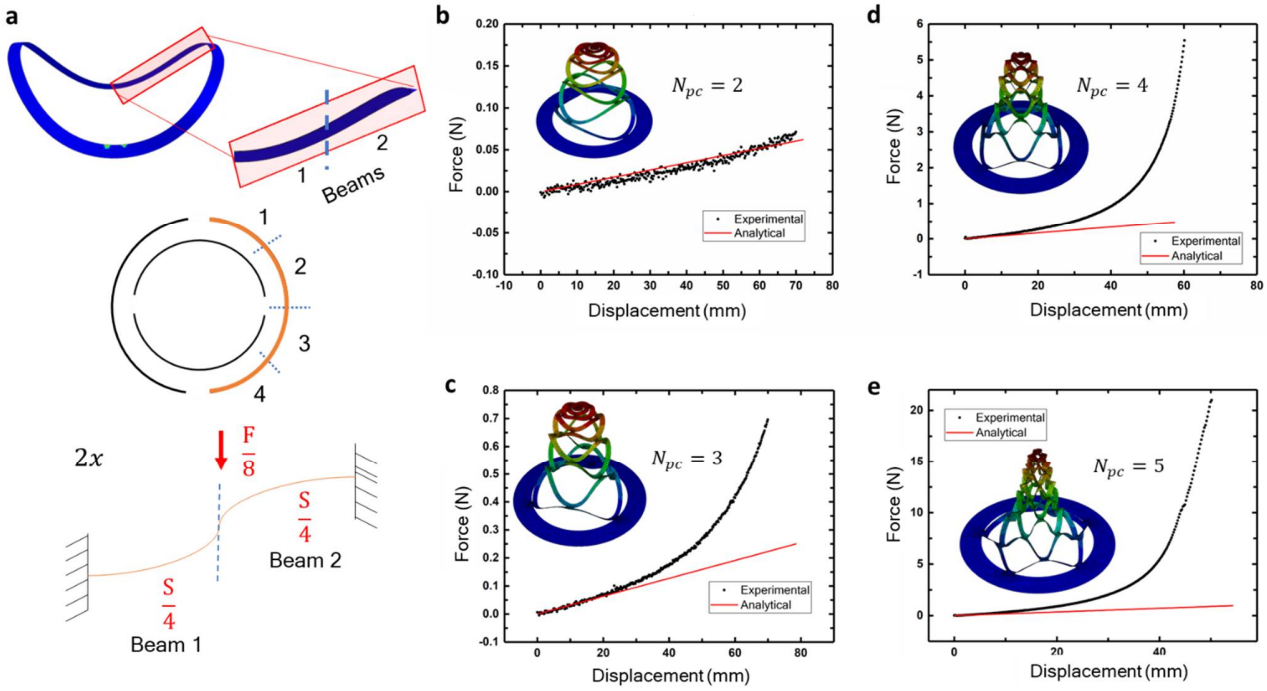

Figure S6. Segments of the deformed ring represented as beams in bending modeled based on the cantilever beam theory. a) For two cuts along the perimeter, part of the ring having a positive slope is represented as two beams and the entire ring is broken into eight beams, so the force applied to one beam is one eighth the total force applied to the entire ring. The experimental results and analytical model are shown (b)-(d) based on the number of cuts along the perimeter with overlaid FEA models displaced by 50 mm.

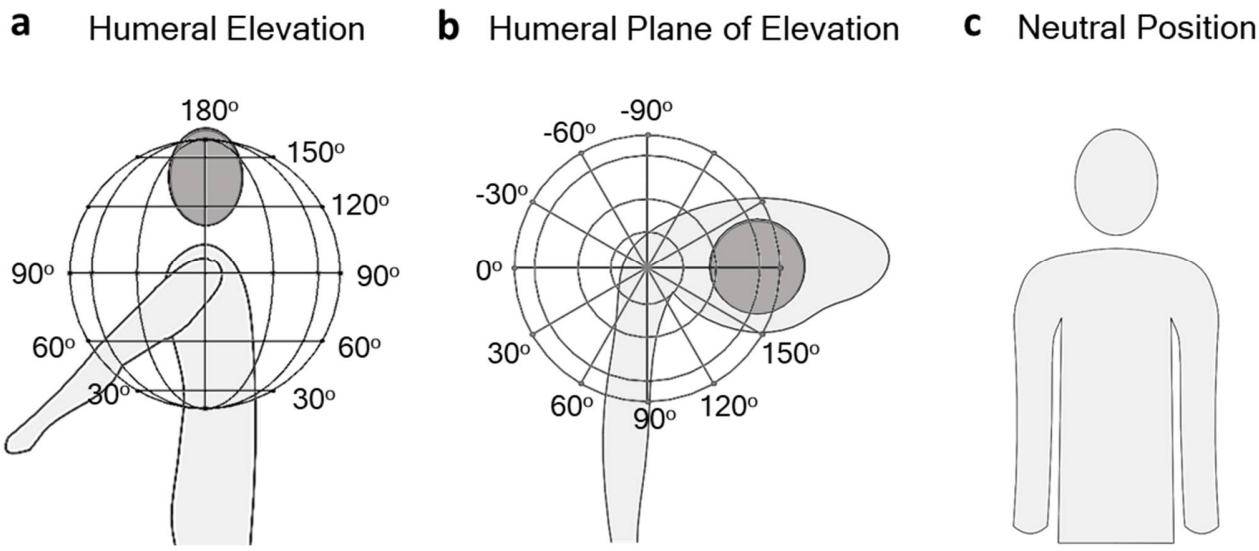

Figure S7. Planes of motion a) humeral elevation angle, (b) humeral plane of elevation, and (c) neutral position of body.

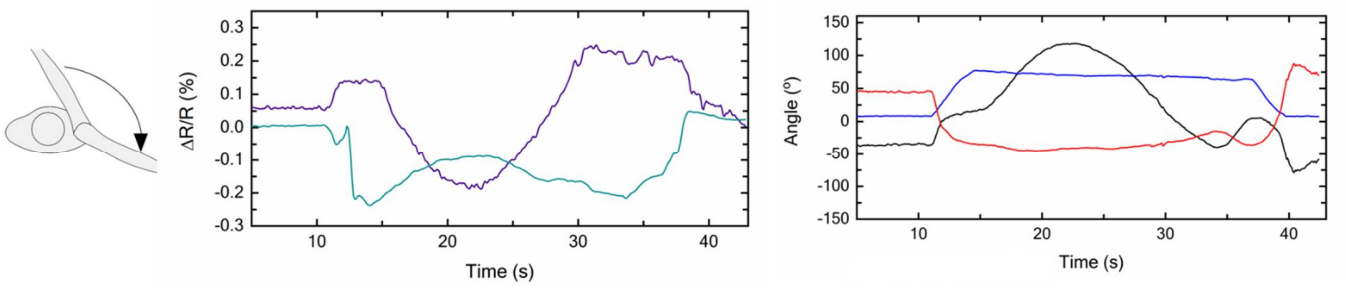

Figure S8. Changes in resistance and corresponding angular positions as the user moves her arm across and behind the body at a constant elevation, arm raised forms 90^{o} from the side of the body.

Table S1. Cut parameters associated with patterns in Figure S1. Radial spacing (*w*), angular spacing (ϕ), and number of cuts along the circumference of the circle (N_{pc}).

	Radial Spacing (*w*) (mm)	**Angular Spacing (ϕ) (°)**	**Number of cuts (N_{pc})**
B	3	10	2
C	5	10	2
D	3	25	2
E	3	10	4